P H Y S I C A L   R E V I E W   L E T T E R S

Inertial Clustering of Particles in High-Reynolds-Number Turbulence

Ewe Wei Saw,[1] Raymond A. Shaw,[1,*] Sathyanarayana Ayyalasomayajula,[2] Patrick Y. Chuang,[3] and Ármann Gylfason[2,†]

[1]*International Collaboration for Turbulence Research and Department of Physics, Michigan Technological University,
Houghton, Michigan 49931, USA*
[2]*International Collaboration for Turbulence Research and Sibley School of Mechanical and Aerospace Engineering,
Cornell University, Ithaca, New York 14853, USA*
[3]*Department of Earth Sciences, University of California Santa Cruz, Santa Cruz, California 95064, USA*

We report experimental evidence of spatial clustering of dense particles in homogenous, isotropic turbulence at high Reynolds numbers. The dissipation-scale clustering becomes stronger as the Stokes number increases and is found to exhibit similarity with respect to the droplet Stokes number over a range of experimental conditions (particle diameter and turbulent energy dissipation rate). These findings are in qualitative agreement with recent theoretical and computational studies of inertial particle clustering in turbulence. Because of the large Reynolds numbers a broad scaling range of particle clustering due to turbulent mixing is present, and the inertial clustering can clearly be distinguished from that due to mixing of fluid particles.

PACS numbers: 47.55.−t, 47.27.Gs, 47.27.Jv, 92.60.Nv

It is a common observation that a "passive" tracer injected nonuniformly into a turbulent flow (e.g., a substance that only marks but does not modify the flow, such as smoke in air or milk in tea) will soon be stirred and mixed by the random vortices in the turbulence until it attains a uniform distribution. Such high mixing power is in fact a hallmark of turbulent flow [1]. One might reasonably ask if the same holds true when the substance is no longer a perfect fluid tracer, such as one that consists of macroscopically discrete particles possessing finite inertia, like the distribution of water droplets in turbulent clouds (e.g., actively convective cumulus clouds). In fact, water droplets with mass density 10^3 times greater than that of air are dynamically stubborn and do not exactly follow the motion of the host fluid. As a result, these "inertial particles" should have a steady state spatial distribution differing from that of a uniform field of fluid particles [2–7].

The inertial clustering phenomenon has implications for a wide range of problems in nonlinear and fluid dynamics, including the formation of rain by droplet collisions in atmospheric clouds [8–10]. Because the droplet collision rate is proportional to droplet density squared, spatial correlations due to inertial clustering can result in accelerated rain formation. Considerable progress has been made in computational and theoretical studies of inertial clustering, but experimental results are sparse [11,12] and the nature of inertial clustering at high Reynolds numbers remains an open problem [13]. Qualitatively, inertial clustering can be understood as the result of particles being centrifuged out of turbulent vortices and thus congregating in regions of high strain [3,5]. Turbulence is a multiscale process in which energy injected at large scales (of order l) "cascades" to progressively smaller scales through nonlinear interactions such as vortex stretching. Over most of these spatial scales, known as the inertial range, fluid

inertia dominates over viscous forces; the scales at which viscosity becomes important lie in the dissipation range. The clustering of inertial particles is significant at dissipation scales and below because it is in this range that turbulent vorticity and accelerations are strongest [9,14,15]. It should be noted, however, that alternate interpretations and approaches exist [16–20], adding impetus to the need for experimental data capable of elucidating mechanisms and constraining theory. To that end, it is the purpose of this Letter to describe an experimental study of inertial clustering and its dependence on particle size and turbulence conditions at high Reynolds numbers.

Suitable quantification of clustering is provided by the particle pair correlation function $\eta(r)$ [5,10], whose magnitude characterizes the strength of clustering at scale r. Intuition on the properties of $\eta(r)$ can be gained by examining how it is calculated in our experiment for one-dimensional sampling of the particle spatial distribution [21]:

$$\eta(r) = \frac{\tilde{Q}(r)/\delta r}{Q/L} - 1, \qquad (1)$$

where $\tilde{Q}(r)$ is the number of particle pairs separated by a distance within $[r - \delta r/2, r + \delta r/2]$, Q is the total number particle pairs in the sample, L is the sample length. Previous theoretical and direct-numerical-simulation studies [6,9,15,22,23] suggest that under ideal conditions (homogenous and isotropic turbulence, single-size particle population, particle-fluid coupling following Stokes's law, dilute particle loading, and negligible role of gravity) $\eta(r)$ satisfies a simple power law [24]:

$$\eta(r) \propto (r/r_K)^{-f(\mathrm{St})}, \qquad (2)$$

where r_K is the Kolmogorov length scale (characterizing

the dissipation range) and $f(\text{St}) > 0$ increases monotonically with St for St < 1. Here, the Stokes number (St) characterizes the particle's inertial response to the flow and is defined as the ratio of the particle inertial response time τ_d to the Kolmogorov time τ_K (coherence time scale for the dissipation range) [1]:

$$\text{St} = \frac{\tau_d}{\tau_K} = \frac{1}{18}\left(\frac{\rho_d}{\rho}\right)\left(\frac{d}{r_K}\right)^2, \qquad (3)$$

where ρ_d is the particle mass density, d is the particle diameter, and the Kolmogorov microscale $r_K = (\nu^3/\varepsilon)^{1/4}$ depends on the kinematic viscosity ν of the fluid (air) and the turbulent kinetic energy dissipation rate ε.

The experimental setup, which is further detailed in the supplementary material [25], consists of a wind tunnel with well-characterized turbulence, sprays for particle generation, and a particle detector. Homogenous and nearly isotropic turbulent flow is generated by a motorized "active grid" capable of achieving high Reynolds number [26–28]. Water droplets are introduced via four spray nozzles, with the resulting size distribution being broad ($\bar{d} = 22$ μm, $\sigma_d = 13$ μm). Downstream, a phase-Doppler interferometer (PDI) [29] simultaneously measures the diameter (d_i), downstream speed (v_i), and arrival time (t_i) of all droplets that traverse its view volume (which has cross section of approximately 150 μm × 210 μm). Table I lists the flow parameters for the various experiments carried out in the wind tunnel: the experiments differ in R_λ and ε, and therefore have different r_K. Each experiment is referred to by a name based on the distance downstream from the active grid (in meters) where measurements are taken and the speed of the fan [in hertz (Hz)] that drives the wind tunnel.

The PDI is stationed far enough downstream ($X = 3$ and 5 m, where X is the distance from the active grid) such that the small scale spatial distribution of the droplets reported here have ample interaction time with the turbulence to

TABLE I. Experiment flow parameters, where R_λ is the Taylor-scale Reynolds number, U is the mean and u is the rms fluctuation of the flow speed along the wind tunnel. The last 4 rows are the droplet diameters (in μm) and corresponding gravitational settling parameters, S_g, for the St bins used in the data analysis.

Experiment	3m-20Hz	3m-30Hz	5m-20Hz	5m-30Hz
R_λ	520	660	440	590
ε (m^2 s^{-3})	1.6	5.4	0.6	2.0
U (m s^{-1})	4.69	6.78	4.59	6.81
u/U	0.17	0.18	0.12	0.13
r_K (μm)	210	150	270	200
St = 0.3	18, 0.14	13, 0.05	23, 0.30	16, 0.10
St = 0.7	27, 0.32	20, 0.13	35, 0.69	25, 0.26
St = 1.1	34, 0.50	25, 0.20	43, 1.04	32, 0.42
St = 1.5	39, 0.66	29, 0.27	51, 1.46	37, 0.56

achieve equilibrium. This follows from the fact that the transit time of droplets is much larger than the Kolmogorov time scale (at least $200\tau_K$; see supplementary material [25] for additional details). To obtain the droplet spatial distribution (x_i) needed for the evaluation of $\eta(r)$ using (1), we adopt a method equivalent to Taylor's frozen turbulence hypothesis [1] in which the time series is converted into a spatial one ($x_i = t_i U$). Within each experiment, the dependence of clustering on particle inertia is studied by selecting droplets from a small range of Stokes numbers St $\pm \Delta$St and then evaluating $\eta(r)$ for that subset of droplets. In practice, ΔSt is chosen such that acceptable counting statistics are obtained. Stokes numbers are calculated using Stokes drag [cf. Eq. (3)], which is accurate to within 10% for the largest droplet diameters used in this study (≈ 50 μm). The uncertainty in this study is dominated strongly by the "shot noise" in the value of $\eta(r)$ due to droplet counting statistics, as detailed in the supplementary material [25].

The essential experimental results on particle clustering are presented in Figs. 1 and 2, which depict the dependence of $\eta(r)$ on $\hat{r} \equiv r/r_K$ for various flow conditions [in log-log coordinates; cf. Eq. (2)]. Figure 1 illustrates how $\eta(r)$ changes with St within a single experiment (3m-30Hz). We note that strong clustering is mainly limited to scales $\hat{r}$ on the order of 10 and below [24], and that clustering is stronger for droplets of larger St. Onset of clustering in the dissipation range and monotonic increase of clustering with St are consistent with theory for St ≪ 1 [6,15]). Within the inertial range, on the order of $10 \lesssim \hat{r} \lesssim 1000$, the correlation functions $\eta(\hat{r})$ show weakly decreasing
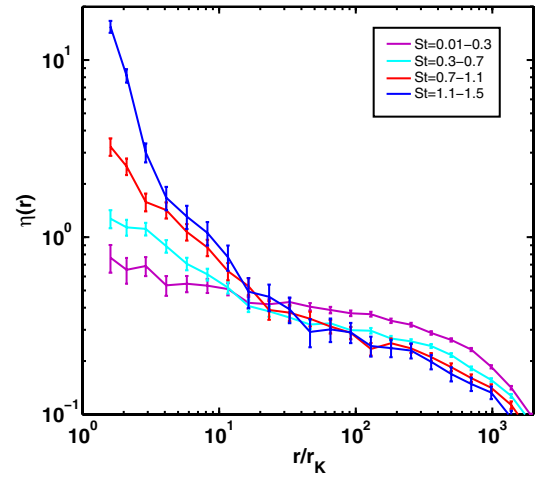

FIG. 1 (color online). $\eta(r)$ versus $\hat{r}$ ($\equiv r/r_K$) with error bars of $2\sigma_{\eta(r)}$, and with $\eta(r)$ parametrized by St from experiment 3m-30Hz. Consistent with theoretical expectations, $\eta(r)$ increases in magnitude with increasing Stokes number in the dissipation range. Each line is $\eta(r)$ calculated from droplets within the specified range of St (from bottom to top corresponding to successively larger St). The errors are evaluated as $2\sigma_{\eta(r)}$ (details in text).
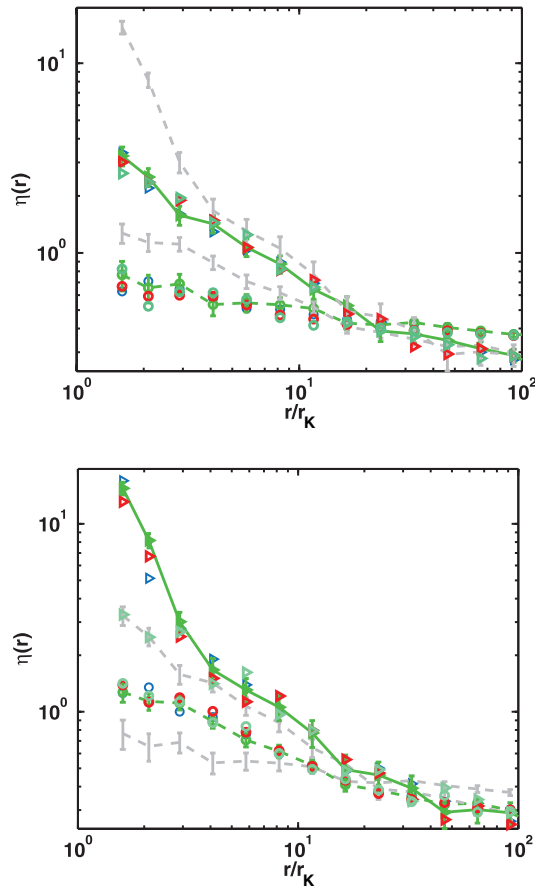
FIG. 2 (color). Stokes-similarity results shown in two panels for clarity. (a) St similarity for droplets with St = 0.01–0.3 (circles) and St = 0.7–1.1 (triangles). Plots for other St groups from Fig. 1, 3m-30Hz, are shown in the background for comparison. The marker colors represent $\eta(r)$ from different experiments (blue, 3m-20Hz; green, 3m-30Hz; red, 5m-20Hz; cyan, 5m-30Hz). (b) St similarity for St = 0.3–0.7 (circles) and St = 1.1.–1.5 (triangles).

clustering with increasing $\hat{r}$, and then fall off more strongly at larger $\hat{r}$. This inertial-range behavior typifies correlations arising from mixing of a passive tracer by turbulence [e.g., $\eta(r)$ scaling as $1 - (r/l)^{2/3}$] (Ref. [30], Sec. 2.9). Essentially, large-scale inhomogeneities in the droplet spatial distribution induced by the spray injection are subsequently stretched and distorted in the turbulent cascade, as the droplets are advected downstream.

Droplets with different diameters but equal Stokes numbers from the experiments are compared in Fig. 2 (zoomed scale), demonstrating "Stokes similarity" consistent with scaling arguments for inertial clustering. The $\eta(r)$ values for the same St range coincide to within the experimental error even though each is obtained from different flow conditions and droplet sizes (see Table I). In obtaining such comparison of the dissipation-range clustering, large-scale correlations resulting from inertial-range mix-

ing must be removed. To that end, the $\eta(r)$ curves in Fig. 2 are normalized such that they coincide in the inertial subrange ($\hat{r} \sim 100$) (see supplementary material [25] for details). Finally, we note that although Stokes similarity is evident in Fig. 2, for one data set a discrepancy is observed for $1.1 < \text{St} < 1.4$, suggesting that the behavior of droplets with St > 1 merits future investigation.

A further observation from Fig. 2 is the apparent power-law dependence of $\eta(r)$ in the dissipation range (for St ≲ 1.1 data). Although this observation is rather tentative given the level of uncertainty and the limited window of resolvable scales showing constant slope, it suggests that the power law is realized even for droplets with finite Stokes number. Theoretically, the power law is valid for St ≪ 1 [see Eq. (2)], but computational work suggests that the power-law dependence continues to hold for St ≲ 1 as well [22], consistent with our results. Detailed theoretical and computational accounting of the more realistic case of a finite range of Stokes numbers (i.e., $\Delta\text{St} > 0$) is still lacking, thus a direct comparison of our results with theory is not possible here. Finally, quantitative comparison of theoretical and measured power-law exponents will require greater resolution at low Stokes numbers since the theory is strictly applicable to St ≪ 1.

Recently Wood and co-workers [12] also addressed inertial clustering in an experiment with $R_\lambda = 230$ and obtained results in qualitative agreement with computational work. We are especially interested, however, in the implications of inertial clustering for cloud droplets and its possible influence on the development of precipitation [10]. For geophysical problems the open question of Reynolds number dependence [13] is crucial, and therefore we have utilized an experimental system allowing us to attain Reynolds numbers approaching 10^3. This leads to a clear separation of scales (i.e., $l/r_K \approx 2000$) and reveals the relative roles of inertial-range mixing and dissipation-range clustering due to droplet inertia. This is critical in allowing comparison between controlled laboratory data such as these, to similar particle-counting measurements in clouds, where turbulence characterization is considerably more difficult [31–34].

Yet to be studied methodically is the role of gravitational settling in inertial clustering. Theoretical findings on this matter are sparse and the problem remains open. Our experiments have large ε relative to many atmospheric clouds, thus the role of gravity is relatively less important. Theoretically, the importance of gravity is expected to scales as the gravitational sedimentation parameter $S_g \equiv \tau_K/\tau_g$, where τ_g is the time required for a droplet to fall over a distance of r_K at its terminal speed. In our experiments, the values of this quantity (cf. Table I) suggest that the role of gravity ranges from small ($S_g \sim 0.01$) to significant, but not dominant ($S_g \sim 1$). However, the observation of Stokes similarity in our results (despite the fact that S_g changes by fivefold to sixfold in each St range)

P H Y S I C A L   R E V I E W   L E T T E R S

*Corresponding author.
rashaw@mtu.edu
†Current address: School of Science and Engineering, Reykjavik University, Reykjavik, Iceland.

[1] H. Tennekes and J. L. Lumley, *A First Course in Turbulence* (MIT, Cambridge, MA, 1972).
[2] M. R. Maxey, J. Fluid Mech. **174**, 441 (1987).
[3] J. K. Eaton and J. R. Fessler, Int. J. Multiphase Flow **20**, 169 (1994).
[4] T. Elperin, N. Kleeorin, and I. Rogachevskii, Phys. Rev. Lett. **77**, 5373 (1996).
[5] S. Sundaram and L. R. Collins, J. Fluid Mech. **335**, 75 (1997).
[6] E. Balkovsky, G. Falkovich, and A. Fouxon, Phys. Rev. Lett. **86**, 2790 (2001).
[7] M. Cencini, J. Bec, L. Biferale, G. Boffetta, A. Celani, A. Lanotte, S. Musacchio, and F. Toschi, J. Turbul. **7**, 1 (2006).
[8] M. Pinsky and A. Khain, Q. J. R. Meteorol. Soc. **123**, 165 (1997).
[9] G. Falkovich, A. Fouxon, and M. G. Stepanov, Nature (London) **419**, 151 (2002).
[10] R. A. Shaw, Annu. Rev. Fluid Mech. **35**, 183 (2003).
[11] A. Aliseda, A. Cartellier, F. Hainaux, and J. C. Lasheras, J. Fluid Mech. **468**, 77 (2002).
[12] A. M. Wood, W. Hwang, and J. K. Eaton, Int. J. Multiphase Flow **31**, 1220 (2005).
[13] L. R. Collins and A. Keswani, New J. Phys. **6**, 119 (2004).
[14] L. P. Wang and M. R. Maxey, J. Fluid Mech. **256**, 27 (1993).
[15] J. Chun, D. L. Koch, S. L. Rani, A. Ahluwalia, and L. R. Collins, J. Fluid Mech. **536**, 219 (2005).
[16] K. Duncan, B. Mehlig, S. Östlund, and M. Wilkinson, Phys. Rev. Lett. **95**, 240602 (2005).
[17] T. Elperin, N. Kleeorin, V. S. L'vov, I. Rogachevskii, and D. Sokoloff, Phys. Rev. E **66**, 036302 (2002).
[18] L. I. Zaichik and V. M. Alipchenkov, Phys. Fluids **15**, 1776 (2003).
[19] S. Ghosh, J. Dávila, J. C. R. Hunt, A. Srdic, H. J. S. Fernando, and P. R. Jonas, Proc. R. Soc. A **461**, 3059 (2005).
[20] L. Chen, S. Goto, and J. C. Vassilicos, J. Fluid Mech. **553**, 143 (2006).
[21] G. L. Holtzer and L. R. Collins, J. Fluid Mech. **459**, 93 (2002).
[22] W. C. Reade and L. R. Collins, Phys. Fluids **12**, 2530 (2000).
[23] A. R. Kerstein and S. K. Krueger, Phys. Rev. E **73**, 025302(R) (2006).
[24] While it is usually stated that the theories apply to the limit $r/r_K \ll 1$, in fact the power-law form is predicted to continue to the correlation scale of velocity gradients. That scale is on the order of $r/r_K \sim 10$; see A. S. Monin and A. M. Yaglom, *Statistical Fluid Mechanics: Mechanics of Turbulence* (MIT, Cambridge, MA, 1975), Vol. II, Sec. 23.4 and Fig. 77; S. G. Saddoughi and S. V. Veeravalli, J. Fluid Mech. **268**, 333 (1994), Sec. 3.2.1 and Fig. 10.
[25] See EPAPS Document No. E-PRLTAO-100-039820 for details on the experimental setup, error analysis, and the data processing. For more information on EPAPS, see http://www.aip.org/pubservs/epaps.html.
[26] S. Ayyalasomayajula, A. Gylfason, L. R. Collins, E. Bodenschatz, and Z. Warhaft, Phys. Rev. Lett. **97**, 144507 (2006).
[27] L. Mydlarski and Z. Warhaft, J. Fluid Mech. **320**, 331 (1996).
[28] L. Mydlarski and Z. Warhaft, J. Fluid Mech. **358**, 135 (1998).
[29] P. Y. Chuang, E. W. Saw, J. D. Small, R. A. Shaw, C. M. Sipperley, G. A. Payne, and W. D. Bachalo, Aerosol Sci. Technol. (to be published).
[30] J. L. Lumley and H. A. Panofsky, *The Structure of Atmospheric Turbulence* (John Wiley & Sons, New York, 1964).
[31] J.-L. Brenguier, T. Bourrianne, A. de Araujo Coelho, J. Isbert, R. Peytavi, D. Trevarin, and P. Weschler, J. Atmos. Ocean. Technol. **15**, 1077 (1998).
[32] A. B. Kostinski and R. A. Shaw, J. Fluid Mech. **434**, 389 (2001).
[33] K. Lehmann, H. Siebert, M. Wendisch, and R. A. Shaw, Tellus, Ser. B **59**, 57 (2007).
[34] M. Pinsky and A. Khain, J. Appl. Meteorol. **42**, 65 (2003).